

Repurposing an Erstwhile Cancer Drug: A Quantitative and Therapeutic Evaluation of Alternative Nanosystems for the Delivery of Colchicine to Solid Tumors

Shifalika Tangutoori¹, Akio Ohta², Samuel Gatley¹ and Robert B. Campbell^{1,3*}

¹Department of Pharmaceutical Sciences, Bouvè College of Health Sciences, Northeastern University, Boston, USA

²New England Inflammation & Tissue Protection Institute, School of Pharmacy, Northeastern University, Boston, USA

³Department of Pharmaceutical Sciences, Massachusetts, MCPHS University, USA

Abstract

Background: Antimitotic drugs represent some of the most popular vascular disrupting agents used today in the fight against cancer. Colchicine is the first known antimitotic alkaloid. The drug binds to tubulin proteins and depolymerizes microtubules. Despite the impressive therapeutic activity as an antimitotic agent, colchicine is fatally toxic when administered to cancer patients intravenously due to its low therapeutic index. This study supports the early development of a relatively safe and target-specific nanoparticle for the IV administration of colchicine to lung tumors.

Methods: For *in vitro* studies, lung cancer (LLC, Chago-k-1 and MCA-205), and endothelial cell lines (MS1-VEGF, HMEC-1) were employed. The qualitative and quantitative analyses of the cytoskeleton and nuclear areas were performed using FITC-labeled β -tubulin antibody; the mean area of cytoskeleton and nucleus per cell was determined by fluorescence microscopy and BIOQUANT. *In vivo*, the biodistribution and therapeutic efficacy studies of the pegylated cationic liposomes (PCLs) were performed in C57BL/6 mice bearing pseudo-orthotopic lung tumors. The biodistribution of colchicine and PCL-colchicine was determined by dual labeling. ¹¹¹In labeled PCLs and ³H-Colchicine were employed to simultaneously track the vehicle and drug, respectively. The therapeutic efficacy was determined by monitoring animal survival.

Results: The disruption of microtubules was most evident when colchicine was loaded in DOTAP-PCLs. We report a ~2 fold ($p=0.0214$, 95% CI is 2.923 to 13.247) increase in the accumulation of PCL-colchicine in tumor-bearing lung compared to the normal lung, resulting in significantly extended survival times in PCL treated group ($p=0.0052$, Log Rank (Mantel-Cox test)).

Conclusions: The PCL-based colchicine-loaded nanosystem can renew the clinical potential of abandoned antimitotic agents such as colchicine. The PCL platform can enable the accumulation of clinically relevant doses of colchicine in solid tumors. This will ensure antimitotic activity while decreasing the uptake of the drug in healthy tissues.

Keywords: Angiogenesis; β -tubulin; Cancer; Cationic liposomes; Colchicine; Endothelial cells; Microtubules; PEG; Tumor vasculature; Vascular disrupting agents

List of Abbreviations

BSA: Bovine Serum Albumin; Chago-k-1: Human Non-Small Cell Lung Cancer Cell Line; DDAB: Didodecyltrimethylammonium Bromide; DIC: Differential Interference Contrast Microscopy; DMEM: Dulbecco's Modified Eagles Medium; DMTAP: Dimyristoyl-3-trimethylammonium Propane; DODAP: Dioleoyl-3-diimethylammonium Propane; DOPC: Dioleoyl Phosphatidylcholine; DOPE: PEG₅₀₀₀: Dioleoylphosphatidyl Ethanolamine: PEG₅₀₀₀; DOTAP: Dioleoyl-3-trimethylammonium Propane; DSTAP: Disteroyl-3-Trimethylammonium Propane; EBM-2: Endothelial Basal Medium; FBS: Fetal Bovine Serum; FITC: Fluorescence Isothiocyanate; FOV: Fields of View; HMEC-1: Human Microvascular Endothelial cells; LD₅₀: Dose of colchicine lethal to 50% of the population; LLC: Lewis Lung Carcinoma Cell Line; MCA-205: Chemically-Induced Fibrosarcoma Cells; MS1-VEGF: Murine Endothelial Cells; PBS: Phosphate Buffered Saline; PCLs: Pegylated Cationic Liposomes; RPMI: Roswell Park Memorial Institute

Introduction

Lung cancer is the leading cause of cancer deaths in the United States, currently contributing to 28% and 26% of all cancer deaths

in males and females, respectively [1]. Various treatment options currently exist, however, the contribution of anti-tubulin agents to cancer chemotherapy is now widely recognized for their broad range of clinical applications [2-6]. The natural alkaloid colchicine, extracted from the stem of saffron meadow (*Colchicum autumnale*), is the first known antitubulin drug than can arrest cellular division at the metaphasic stage [7].

The anti-mitotic effect of colchicine was exploited for the treatment of carcinomas as early as 1930's [8]. Early *in vivo* studies showed that colchicine induced hemorrhagic necrosis and anti-vascular effects in tumors [9,10]. Colchicine has since been shown to be an effective

***Corresponding author:** Robert Campbell, Associate Professor, Department of Pharmaceutical Sciences, MCPHS University, 19 Foster Street Worcester, Massachusetts 01608-1715, USA, Tel: 508.373.5740; Fax: 508.890.5618; E-mail: robert.campbell@mcpchs.edu

Received May 13, 2014; Accepted June 28, 2014; Published June 30, 2014

Citation: Tangutoori S, Ohta A, Gatley S, Campbell RB (2014) Repurposing an Erstwhile Cancer Drug: A Quantitative and Therapeutic Evaluation of Alternative Nanosystems for the Delivery of Colchicine to Solid Tumors. J Cancer Sci Ther 6: 236-246. doi:10.4172/1948-5956.1000277

Copyright: © 2014 Tangutoori S, et al. This is an open-access article distributed under the terms of the Creative Commons Attribution License, which permits unrestricted use, distribution, and reproduction in any medium, provided the original author and source are credited.

inhibitor of angiogenesis, but only when administered above the maximum tolerated dose [11]. The risk associated with intravenous use of colchicine is due to widely variable patient responses to therapy, and metronomic doses required for effective disease management [12,13]. True to its poisonous nature, many suicides and homicides resulted due to the consumption of doses higher than those prescribed [12,14-18]. Currently, the ISMP (Institute for Safe Medication Practices) has listed the intravenous use of colchicine as a high toxicity-alert medication [19,20].

In general, the α/β tubulin heterodimers, polymerize into dynamically unstable microtubules, which play an important role in various sub-cellular motility functions, including the events during spindle formation and chromosomal rearrangements during mitosis [19]. Mechanistically, colchicine binds to the interface of α/β tubulin heterodimers and thus inhibits all the subsequent functions in the cancer cell. Colchicine poisoning occurs due to its large volume of distribution, and its potent antimitotic activity towards every non-specific mitotic cell it encounters. Clinical indications of colchicine poisoning are typically anaplastic anemia accompanied by high fever, loss of scalp hair, severe agranulocytic leucopenia, hemorrhage and multisystem failure within 24 to 48 hours of acute over-dosage [8,15]. Hence, efforts to improve targeted delivery of colchicine to lung tumors represent a promising clinical approach [21].

Nanoliposome is a well characterized platform used to deliver many toxic chemotherapeutic drugs [22]. Based on previous works, we postulated that the synthetic cationic lipids (i.e., DOTAP, DODAP, DDAB, DMTAP, DSTAP) are potentially useful in the development of colchicine nanoliposomal formulations for cancer therapy [23,24]. These second generation liposomes have previously been used to selectively target drugs to tumor endothelia [21,25]. We now report the early development and evaluation of Pegylated Cationic Liposomal-colchicine (PCL-colchicine) to achieve superior and selective pulmonary targeting. This investigation details the qualitative and quantitative analyses *in vitro*, and biodistribution and efficacy evaluation studies performed on a pulmonary metastatic tumor model of fibrosarcoma.

Methods

Preparation of nanoliposomes

All lipids were purchased from Avanti Polar Lipids (Alabaster, AL). Liposomes were prepared as previously reported [26,27]. The PCL-colchicine was prepared at 3 and 10 mole% concentrations for *in vitro* and *in vivo* studies (Table S2). A lipid mixture consisting of DOPC: Cationic lipid: Cholesterol: DOPE-PEG₅₀₀₀ (35:50:10:5) was evaporated to dryness at 42°C with the aid of a rotary evaporator to obtain a thin lipid film. Any residual organic solvent was removed by freeze drying the lipid film for an additional 2 hrs using Labconco freeze dryer (Labconco Corporation, Kansas City, MO), followed by hydration and PCL size manipulation as previously reported [28].

Cell lines

LLC, MS1-VEGF [29], Chago-k-1 [30], HMEC-1 [31,32] and maintenance media DMEM, RPMI 1640, EBM-2, VEGF and hFGF-b, and FBS were all purchased from ATCC (American Type Culture Collection, Manassas, VA). PBS 1X was purchased from Cambrex, NJ. MCA-205 [33] was a gift in kind from New England Inflammation & Tissue Protection Institute, Northeastern University (NU), Boston, MA.

Analysis of cytoskeleton disruption using PCL-colchicine

Slow Fade® Gold antifade reagent with DAPI was purchased from Molecular Probes (Invitrogen Life Technologies, Carlsbad, California). Monoclonal Anti β tubulin FITC conjugate and purified mouse immunoglobulin (F 2043) were purchased from Sigma Aldrich (St. Louis, MO). Ammonium acetate and BSA were purchased from Sigma Aldrich (St. Louis, MO). Fluorescence microscopic analyses were carried out using a BX61 W1 Olympus fluorescence microscope from Optical Analysis Corporation (Melville, NY).

Cells were seeded at a density of 5×10^5 onto sterile coverslips in a 6 well plate (Corning, NY). After 24 hrs of incubation at 37°C free drug or liposomal drug was added to selected wells. The well plate was incubated for an additional 24 hrs after which the coverslips were prepared for mounting. Cell fixation and staining with antibody was performed according to specifications provided with the MSDS of FITC-conjugated β tubulin antibody. Briefly, the coverslips were washed twice with 1X PBS to remove cellular debris and then fixed with cold absolute methanol. Coverslips were then incubated at -20°C for 10 min. The methanol was washed off with cold acetone and the cells were rehydrated in 1X PBS for at least 30 min. The rehydrated cells were then incubated with FITC-conjugated β -tubulin antibody for 1 hr, suitably diluted with 1X PBS containing 1% BSA. A working dilution of 1:25 was used. Excess antibody was removed with 1X PBS, and samples were mounted onto a glass slide using Slowfade® Gold antifade reagent DAPI as the mounting media. The images were randomly selected at five different fields of view (FOV). DIC microscopy was used to observe cell shape and morphology prior to obtaining all fluorescence images. The FITC and DAPI images were merged to observe the area of cytoskeleton and nucleus using LLC and MS1-VEGF cell lines. All images were captured at 40X magnification using a BX61 W1 Olympus Fluorescence microscope from Optical Analysis Corporation (Melville, NY).

BIOQUANT for quantitative analysis

BIOQUANT (Image Analysis Corporation) was used to quantify the merged images of the cell nucleus and cytoskeleton. Images were selected randomly at five different FOV on the coverslip. Areas with a fixed threshold of fluorescence intensities for FITC (cytoskeleton) and DAPI (nucleus) were selected and measured (Figure 1). We determined the total number of cells in each field, and the area occupied per cell. Mean cytoskeleton and nuclear areas per cell was plotted as a scatter plot. Each dot in the plot represents the Mean \pm 95% CI of single field in the cell sample. Statistics were performed using one way ANOVA (Graph Pad Prism 5) at a significance level of 0.05, and the Bonferroni post hoc test was used to compare pairs of column in the study.

Animal studies: All of the studies involving animals were performed in accordance with NU-IACUC policies and procedures. C57BL/6 female mice, 8 wks old, weighing ~20 gm, were purchased from Charles River Laboratories Inc. (Wilmington, MA). The radioactive isotopes ¹¹¹In, ³H-colchicine, Solvable™, UltimaGold™ XR used for the biodistribution studies were purchased from PerkinElmer Inc (Waltham, MA). Tissue distribution and therapeutic efficacy studies of formulated and free drug were carried out in C57BL/6 female mice.

Generation of pulmonary metastatic tumor nodules: A well characterized pulmonary metastatic tumor model was developed in female C57BL6 mice as described previously using MCA-205 cells [34]. This pseudo-orthotopic model has been shown to reliably produce pulmonary metastases that can be visualized by microscopic

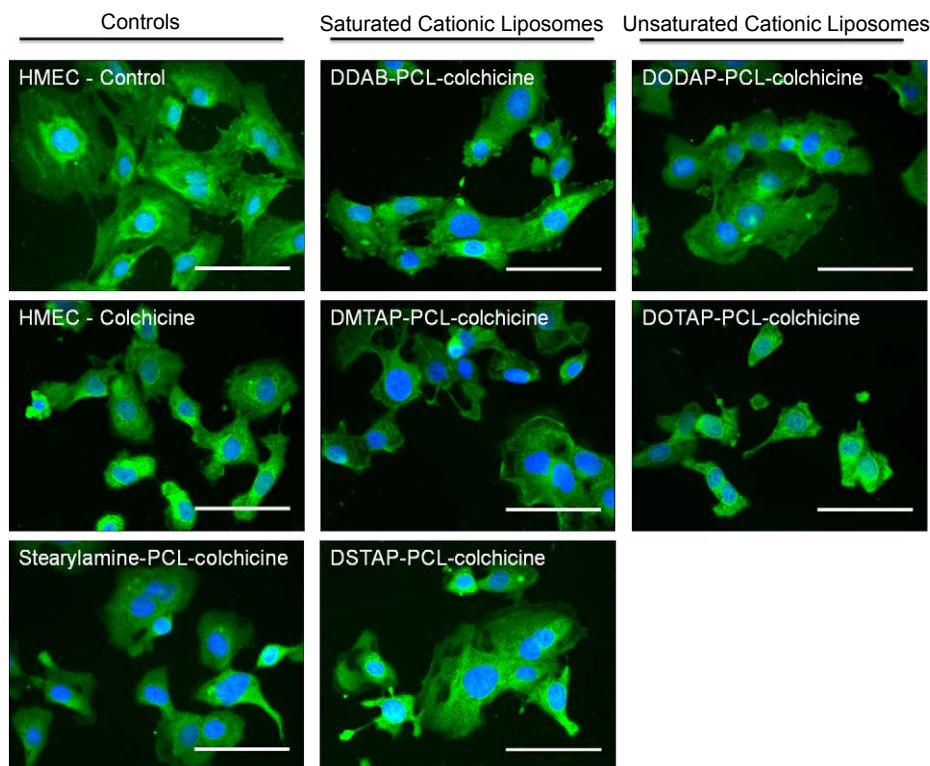


Figure 1: Fluorescence images of endothelial cell, HMEC-1, 24 hrs following exposure to colchicine (free drug) or various PCLs (with colchicine). The images show qualitative effect of different cationic lipids of PCLs on cytoskeleton (green) and the nucleus (blue) cell areas. Images were captured using 40X magnification. Magnification bar = 20 μ m.

evaluation. Briefly, 3×10^5 MCA-205 cells were injected via tail vein into mice and the lungs were harvested at various stages of tumor growth (Table 1 and 2). Mice were anesthetized with ketamine-xylazine (i.p. 9 mg/100 g-0.9-100 g), and excessive inhalation of 5% Isoflourane was used to euthanize the mice

Biodistribution of dual radiolabeled ^{111}In PCL (^3H -Colchicine)

Synthesis of dual radiolabeled [^{111}In PCL (^3H -Colchicine)]: To establish the biodistribution profile of colchicine and PCL-colchicine, two stable radioactive isotopes were employed. PCLs labeled with ^{111}In have been used to detect the path followed by PCLs *in vivo* [35]. Back in 1930's, ^3H -colchicine and ^{14}C -colchicine were used for tracking the drug in various tissues in mice [36,37]. Hence, we formulated the PCL-colchicine using two different radioisotopes. ^{111}In and ^3H were used for tracking PCLs and colchicine, respectively. Unlabeled colchicine was added to trace amounts (5 $\mu\text{Ci}/\text{mouse}$) of ^3H -colchicine to maintain the required drug to lipid ratio with comparable drug loaded. ^{111}In labeling was carried out as described previously [35,38]. Briefly, the required lipids including DTPA-DOPE at 5 mole% were added and a thin film was generated by rotary evaporation. The film was hydrated in (1X) PBS overnight in warm water bath to produce PCLs. The ^3H -colchicine-PCL was acidified using citric acid buffer (pH-4.5), and labeled with ^{111}In (2 $\mu\text{Ci}/\text{mouse}$). At pH 4.5 the ^{111}In was covalently attached to the DTPA in the PCL bilayer. Excess and unbound ^{111}In was separated from the formulation by dialysis overnight in 4L of HEPES buffer (pH 7.4). For free drug, 50 μCi of ^3H - colchicine (from stock of 60-87 Ci/mmol), was measured out, diluted in PBS and injected into mice *via* tail vein.

Biodistribution studies-study design: To study the infiltration of drug in the tumor nodules at various stages of development, tumor

cells were injected on different days and the formulations on a fixed (the same) day. Tumor cells were injected at 1, 5 and 8 days to generate the tumors that were 12, 8 and 5 days old (Groups 3-5), respectively, on the day of treatment (Table-1). One mouse from every group was euthanized, and the lungs were harvested to assess metastasis.

Analysis of ^{111}In labeled PCL accumulation

Measurement of ^{111}In labeled PCLs was carried as explained elsewhere [27]. Briefly, after the mice were sacrificed, various organs including blood, liver, spleen, tail, kidney, lung/tumor and heart were harvested in groups 2-5 and collected into pre-weighed test tubes. The half-life of ^{111}In is 2.8 days, predominantly emitting high energy gamma radiations. The amount of radioactivity thus retained by individual organs was quantified as counts *per minute* (CPMs) using a Beckman 5500B gamma counter (Beckmann instruments, Fullerton, CA), and the amount of the accumulated radioactivity *per gram* of tissue was calculated (% D/M). The radioactivity retained by the tumor-bearing lung was compared with the healthy lung controls.

Analysis of ^3H -colchicine accumulation: The ^3H measurements were acquired based in part on previous reports using radioactive colchicine to determine organ-specific uptake [36,37]. The protocol was modified to meet the goals of the present study. After the mice were sacrificed, various organs were harvested for all groups, and organs were collected into pre-weighed scintillation vials. The half-life of ^3H is 12.3 years, emitting low energy β radiations. To rule out the interference of gamma radiations of the ^{111}In during the ^3H measurements, the tissue samples collected were stored at 4°C for at least 20 days ($10 t_{0.5}$ of ^{111}In) to allow for sufficient ^{111}In decay. The tissue samples were subsequently digested with Solvable™ (Perkin Elmer,

Group	Day of Tumor Injection	Age of tumor (days old)	Single i.v. injection received on day 12 (100 c.c)	Radiolabels Analyzed
1	Control-No tumor	N/A	³ H-colchicine	³ H
2	Control-No tumor	N/A	[¹¹¹ In PCL (³ H colchicine)]	¹¹¹ In and ³ H
3	Day 7	5	[¹¹¹ In PCL (³ H colchicine)]	¹¹¹ In and ³ H
4	Day 4	8	[¹¹¹ In PCL (³ H colchicine)]	¹¹¹ In and ³ H
5	Day 1	12	[¹¹¹ In PCL (³ H colchicine)]	¹¹¹ In and ³ H
6	Day 1	12	³ H-colchicine	³ H

Table 1: Biodistribution study design.

Group	Days of treatment	Dose of drug (mg/ kg)	# of mice per group
1 Untreated controls	-	-	5
2 Colchicine treated	9,12,15	2, 2, 4	5
3 PCL-Colchicine treated	9,12,15	2, 2, 4	5

Table 2: Experimental Design for therapeutic response survival study.

Boston, MA), an aqueous based solubilizer. The highly perfused tissues (i.e., liver, lung, heart, and blood) were treated with 10% H₂O₂ overnight to decolorize dark brown color owing to the blood retention in these tissues. Measures were taken to prevent any escape of tritiated water due to oxidation reactions related to hydrogen peroxide. After all the samples were sufficiently decolorized (light yellowish tinge), 10 mL of liquid scintillation fluid, Ultima Gold™ XR (Perkin Elmer, Boston, MA) was added to each vial, the samples were stored in dark overnight and the following day the CPM's were measured in liquid scintillation counter (Beckman Coulter™, LS-6500 Scintillation Systems, Fullerton, CA). The raw CPM's were used to calculate the % injected dose per gram of the tissue sample collected (% D/G). The radioactivity retained by the tumor-bearing lung was compared with the healthy lung tissue control groups. The distribution profile of free colchicine and PCL-colchicine was also compared.

Therapeutic response -survival studies

Study design: The animal survival study was performed using the pulmonary pseudo-metastatic model. The MCA-205 cells (3x10⁵) were injected via tail vein on day 1. The tumor-bearing mice were separated into 3 different experimental groups. Colchicine or PCL-colchicine was administered on 9, 12 and 15 days following the injection of tumor cells (Table-2). All mice were monitored daily for changes in body weight. To visualize the tumor nodules the lungs were harvested and fixed in Fakete's fixing solution. The Kaplan-meier curves were generated using Graph Pad Prism 5 (Graph Pad Prism software, Inc, La Jolla, CA).

Imaging of tumor nodules: Once the mice were sacrificed they were dissected at the tracheal region, and the diaphragm was removed to clearly expose the lungs. A small nick was made on the trachea and 15% black India ink (Higgins™, Boston, MA) was injected retro-tracheally until the lungs were inflated to their full volume. The lungs insufflated with ink were now black providing a counterstain for the white tumor nodules on the surface. Lungs were then harvested, washed in distilled water to remove excess ink or blood and fixed overnight in Fakete's fixing solution [34]. An *in vivo* imaging microscope (Fisher Scientific, 4.5X) was used to capture the images of the harvested lungs.

Statistical analysis

Statistical analyses were carried out using one way ANOVA with bonforroni post hoc test, log rank Mantel-Cox test (for Kaplan Meier curves) and two tailed t-tests at α=0.05 with 95% CI values as errors.

GraphPad Prism 5 was used to assign the significant values as * p<0.05, ** p<0.001, *** p<0.0001 and to report the 95% confidence intervals.

Results

DOTAP-PCL-colchicine qualitatively altered the cytoskeletal area of endothelial cells to the greatest extent

PCL-colchicine was optimized to increase the potential for tumor vascular disruption. We screened for the synthetic cationic lipid most capable of inducing significant structural changes in endothelial cells when employed in the preparation of PCL-colchicine. HMEC-1 (the endothelial cellular model) was exposed to the various PCL-colchicine formulations composed of both saturated and unsaturated cationic lipids. We analyzed qualitative changes in the cytoskeleton. Qualitatively, DOTAP-PCL-colchicine was the most effective among all the preparations evaluated. The effect of DOTAP-PCL-colchicine was similar also to the effect of free colchicine. This can be attributed to the spacio-temporal availability of higher concentration of the drug, possibly due to relatively rapid release of colchicine when delivered via unsaturated DOTAP-PCLs. In comparison to other PCL varieties, DOTAP was the most effective at altering the structural and morphological properties of the HMEC-1 cells (Figure 2).

PCL-colchicine induced significant quantitative changes to the cytoskeletal area of endothelial cells

Since colchicine and PCL-colchicine altered cell morphology, fluorescence microscopy was next used to quantify the extent of cytoskeletal disruption (Figures 1,3). The results from this study revealed that free colchicine reduced the cytoskeleton area of the endothelial cells without altering the nuclear area. We determined that HMEC-1 had the greatest cytoskeleton area *per cell* (Figure 4E) (1946 ± 306), which was significantly reduced following exposure to colchicine (1073 ± 390, 95% CI-512 to 1234). MS1-VEGF (1692 ± 425), followed the same trend, and exposure to free drug reduced the area to 590 ± 265 (95% CI-276 to 955). Both endothelial cells showed significant decrease in cytoskeleton area *per cell* when compared to the effect of free colchicine (232 ± 173, 95% CI-1033 to 1839) (Figure 3, 4A, 4C).

In cancer cellular models evaluated, PCL-colchicine significantly altered both the cytoskeleton and nuclear areas *per cell* in comparison to untreated cells, except for MCA-205 (Figure 1). Although promising, the qualitative effect observed in cytoskeletal disruption of MCA-205 was not translated quantitatively since there was no significant difference observed compared to the untreated samples (Figure 1E,1F). This can be attributed to several factors including the inherent resistance of the cell line to cytotoxic drug therapy.

Effective delivery and biodistribution profile of PCL-loaded colchicine

We next evaluated the therapeutic effect of PCL-colchicine in a pulmonary metastatic model of MCA-205, as this cell line was derived from metastatic lung cancer. Our rationale was that, the MCA-205 tumor model reliably induces metastatic nodules in the female C57BL6 mice, and is the most 6 k¹ resistant cell line of the many evaluated in this study to the effects of colchicine. In order to determine the changes in the biodistribution profile due to altered pharmacokinetics of the PCL-colchicine, we simultaneously tracked PCL-colchicine or colchicine using ¹¹¹In and ³H isotopes, three hours following a single i.v. injection. We determined that recovery of ¹¹¹In PCL and ³H colchicine in the liver (~40-58%) was the highest among all of the tissues evaluated in the PCL-colchicine treated group. The recovery of both labels from

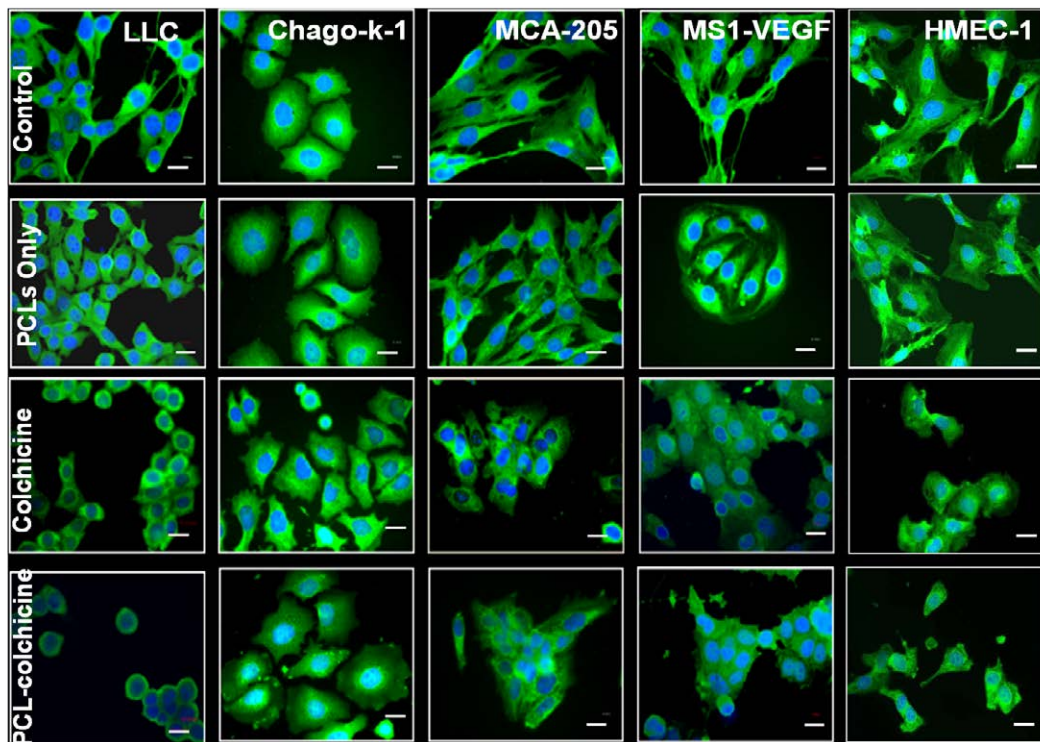


Figure 2: The fluorescence images show the qualitative effect of DOTAP-PCLs, free colchicine and DOTAP-PCL-colchicine against various cancer and endothelial cell lines. The cytoskeleton (green) and nucleus (blue) of the cell were captured using 40X magnification. Magnification bar = 7 μ m.

the same site suggests that the carrier and the drug co-exist (Figure 5A and 5B). The recovery of ^3H label from blood and tumor in PCL-colchicine treated mice was ~10-18% and 10-20% of the injected dose, respectively. The accumulation of the label gradually increased with tumor age (Figure 5B).

The lung to blood ratio in healthy tissue and in tumor-bearing mice treated with PCL-colchicine and colchicine showed ratios of 0.7 and 1.6, respectively. The >2 fold decrease of accumulation in healthy lung compared to the tumor group suggests minimal potential off-targeting effects of PCLs (Figure 6F). In contrast, there was minimal difference in free colchicine accumulation between healthy lungs and in the tumor (Figure 6E). The experimental findings support enhanced tumor targeting in the lung (as supported by a ~10 fold increase in tumor uptake over free drug treated group), and a favorable decrease in non-specific accumulation in healthy lung tissue (Figure 6B).

PCL-colchicine uptake positively correlated with tumor size and age

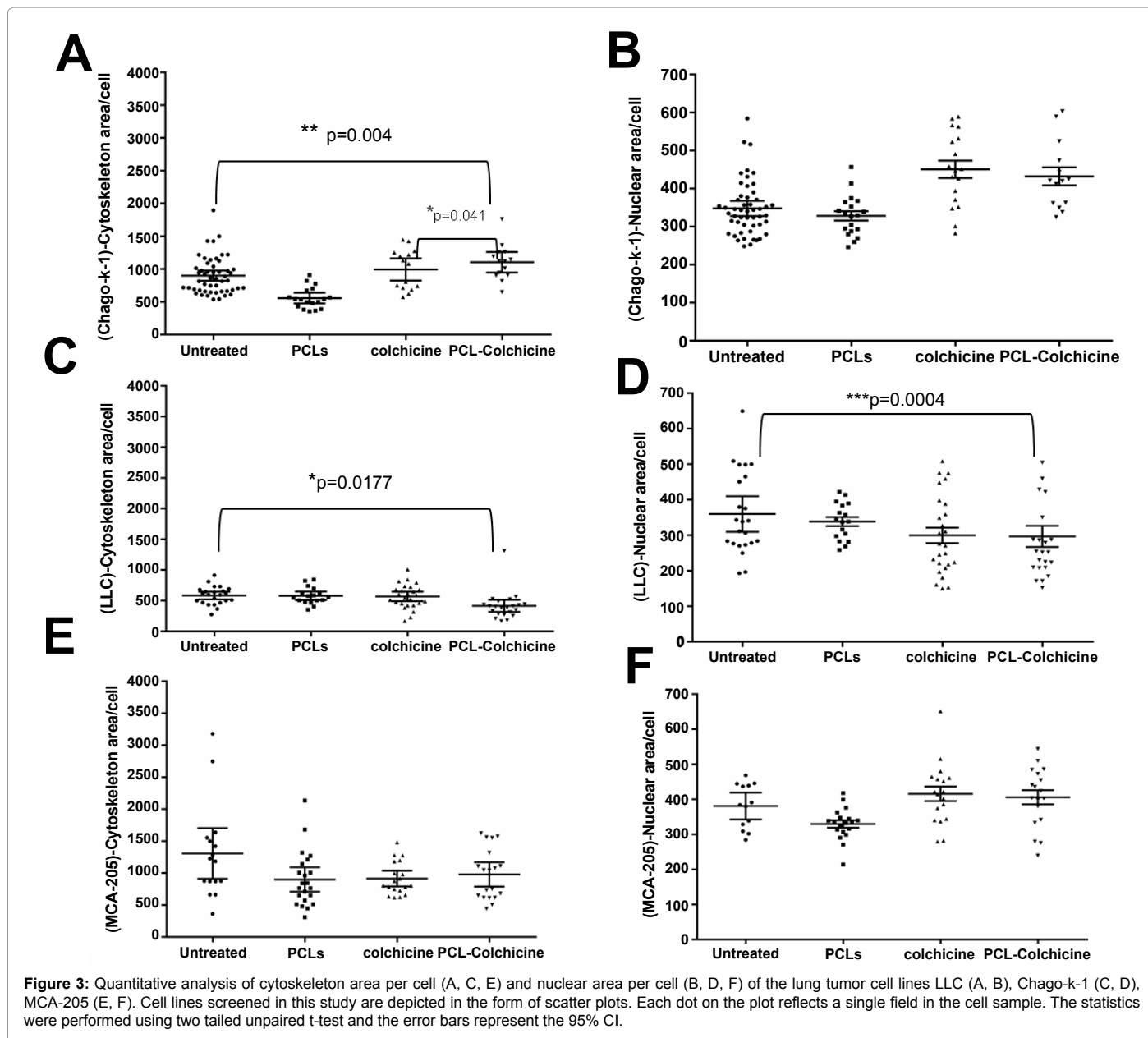
We next evaluated the uptake of PCL-colchicine as a function of tumor burden size/age. The tumors were selected at various stages of growth, and PCL-colchicine was administered via tail vein injection (Figure 6A,6D). We observed a higher tumor to blood ratio in advanced tumors (8 and 12 day), when compared to no tumor group or early stages of tumor development (day 5). The group consisting of 12 day old tumors revealed a significantly higher accumulation of the drug (19% of injected dose) when compared to day 5 (~11% of injected dose), and no tumor (~10% of injected dose). The experimental finding suggested that the overall drug recovery by the tumor mass increased with tumor age (Figure 6C).

PCL-colchicine significantly enhanced survival of tumor-bearing mice

We next determined the therapeutic effect of PCL-colchicine compared to the colchicine treatment. The Kaplan Meier survival curves were used to demonstrate the therapeutic benefit of formulating colchicine in PCLs. The tumor nodules in the untreated control group were larger and greater in number compared to treated groups (Figure 7A). The specific observations are summarized in Table S3. The PCL-colchicine treated groups showed 80% survival on day 23, 40% survival on day 25 and 20% survival on day 29. Therefore, PCLs significantly prolonged effect of colchicine and hence the animal survival compared to other groups (Figure 7B). By day 21, the untreated group showed severe respiratory distress. The mice were extremely moribund, and experienced severe body weight loss (Figure 7C). Following two injections of 2 mg/kg (0.05mg/mouse/injection) in the free and PCL-colchicine treated groups, the mice initially displayed weight loss, but eventually showed signs of recovery (Figure 7D,7E). The third dose was administered to the two groups at 4 mg/kg (0.1 mg/mouse/injection) on day 15. Again, a drastic decrease in the body weight was observed initially followed by a period of recovery. Approximately 48 hours following the final injection, >20% body weight loss was observed in the entire free drug treatment group (Figure 7D), and the mice were subsequently removed from the study according to IACUC regulations. Although the PCL-colchicine showed an initial decrease in body weight (Figure 7E), only one mouse from this group reached the 20% weight loss limit, the remaining subjects demonstrated definite signs of recovery.

Discussion

Colchicine is a potent alkaloid with a highly impressive antimitotic



profile. The drug is currently employed for the treatment of gouty arthritis [7,17], familial mediterranean fever [39] and other vascular-dependent diseases [3,5,6]. The systemic administration of colchicine is not deemed clinically safe due to toxic effects exerted against various tissues. PCLs offer an attractive array of benefits to encapsulate and deliver the toxic drugs like colchicine, including preferential tumor vascular targeting [40].

The structural and chemical differences of various cationic lipids strongly influence physicochemical characteristics of PCLs such as particle size, zeta potential, loading efficiency of the drug and overall extent of liposome uptake [26,28]. Cationic lipids are uniquely identified by their acyl chain length, head group composition, degree of chain saturation, phase transition temperature (T_m) and the spatial arrangement of the head and tail groups in relation to the other lipids. These properties ultimately govern the stability and targeting efficiency

of the eventual formulation [25,41]. The prerequisites for an ideal drug carrier for tumor vascular targeting are particle size (ranging from 100-200 nm), zeta potential (ranging from 20-25 mv) and the capacity for incorporating and delivering the drug payload to desired locations [41]. For any PCL another important consideration is to strike the right balance between the cationic surface charge, and partial shielding of the cationic charge potential afforded by PEG [42]. Therefore, to maximize vascular targeting efficiency we evaluated PCLs as a function of cationic lipid content and type, varied degree of saturation and unsaturation, considered the amount of PEG to employ, the loading efficiency and drug to lipid ratios [25,27,38,40,43,44].

We achieved a loading efficiency of ~80% of the initial drug concentration, the highest degree of loading reported for colchicine in nanoparticle platforms to date. The degree of incorporation is highly dependent on methodology and is lipid-composition dependent [45-

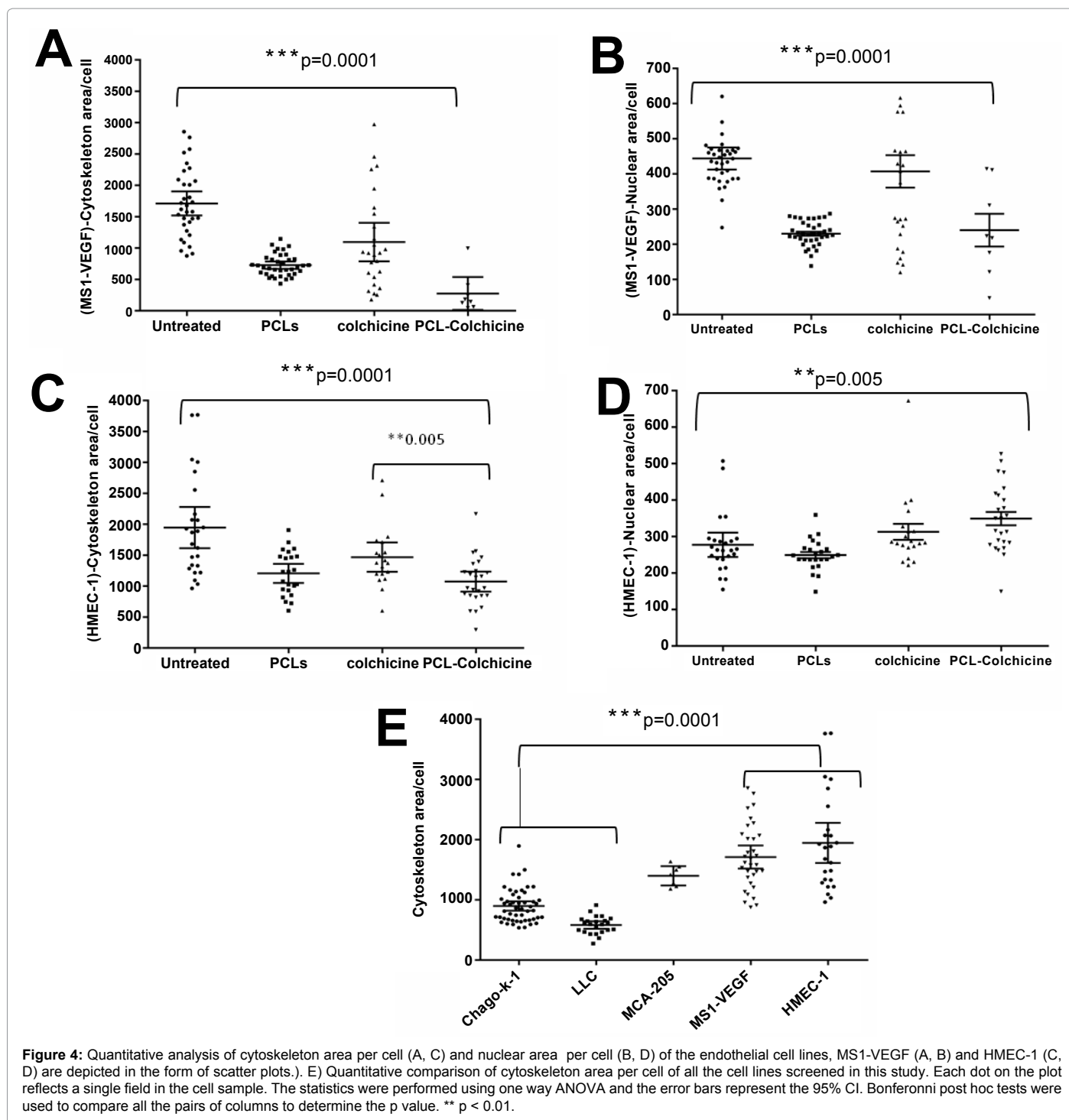


Figure 4: Quantitative analysis of cytoskeleton area per cell (A, C) and nuclear area per cell (B, D) of the endothelial cell lines, MS1-VEGF (A, B) and HMEC-1 (C, D) are depicted in the form of scatter plots. E) Quantitative comparison of cytoskeleton area per cell of all the cell lines screened in this study. Each dot on the plot reflects a single field in the cell sample. The statistics were performed using one way ANOVA and the error bars represent the 95% CI. Bonferonni post hoc tests were used to compare all the pairs of columns to determine the p value. ** p < 0.01.

49]. This finding was further supported by the several week long stability experiments involving the various PCL-colchicine formulations (Figure-S1).

Colchicine exerted a *cytostatic* effect *in vitro*. The sigmoidal dose response curve typically associated with most *cytotoxic* drug agents was not observed against the select cell lines in the dose range evaluated. In addition, the IC_{50} values were not obtained except for HMEC-1 cells (Figure S2). On the basis of the doubling time studies, which

did not necessarily correlate with the drug effect, the findings suggest that rapidly dividing cells may not be essential to achieve a desired colchicine drug action.

The physical properties of colchicine are amphiphilic in nature. The drug is soluble in PBS, methanol and in chloroform at the concentrations employed. For this reason, colchicine incorporated to some extent in both the lipid bilayer and in the aqueous core. Given the ability of second generation cationic lipids to form relatively stable

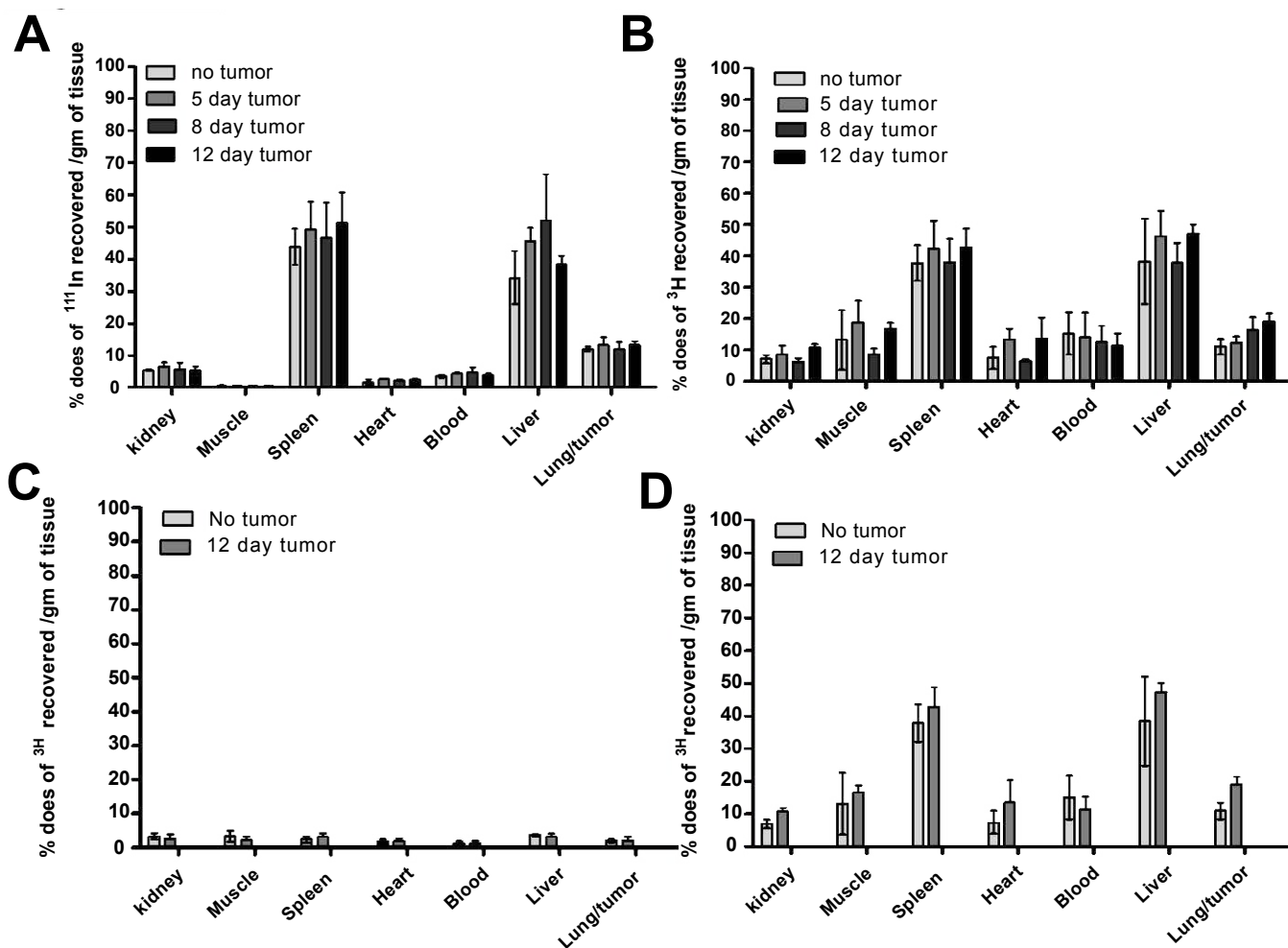
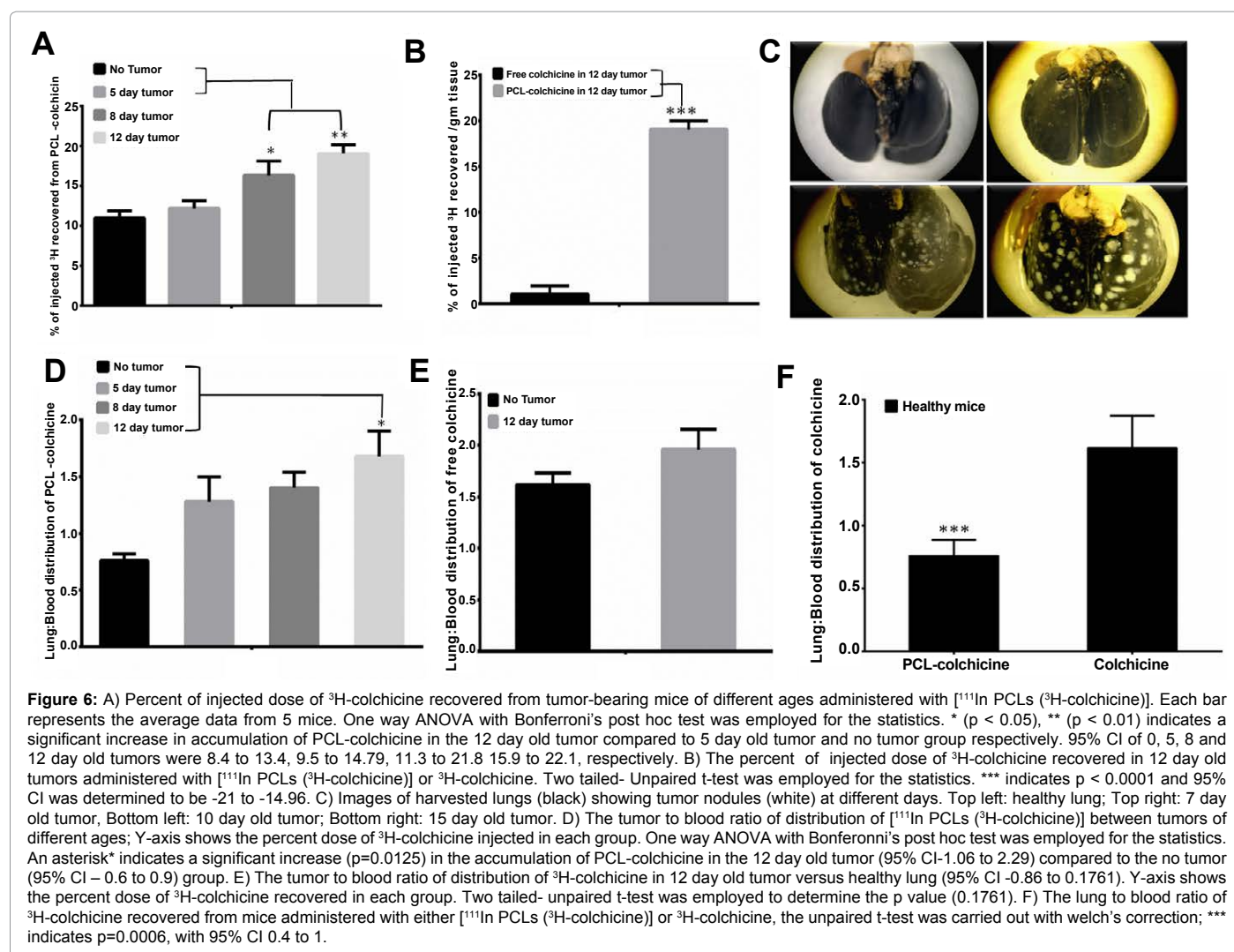


Figure 5: Biodistribution studies using a dual labeling approach: The Y-axis represents the percent dose of ^3H isotope recovered per gram of tissue, 3 hours following i.v. administration of either the [^{111}In PCLs (^3H -colchicine)] or ^3H -colchicine. ^{111}In was used to track the PCLs (A), and ^3H was used to track the colchicine incorporated in PCLs (B). As measured by this dual radiolabeling approach, A and B show co-localization of ^{111}In and ^3H representing PCLs and colchicine, respectively in PCL-colchicine treated mice. C and D show biodistribution of [^{111}In PCLs (^3H -colchicine)] in tumor-bearing mice in comparison to free drug, ^3H -colchicine. Y-axis shows the percent dose of ^3H isotope recovered per gram of tissue for ^3H -colchicine treated mice (C) and PCL- ^3H -colchicine treated mice (D).

liposome bilayers this produced a higher degree of drug loaded in the PCLs, and hence, a greater drug payload was delivered to (and retained by) the target cells. This effect can be observed from the images acquired by fluorescence microscopy. Given that the decrease in the percent of cell viability was significant following treatment with PCL-colchicine (Figure S3), the total cellular surface area might represent an understudied yet important fundamental pre-requisite for optimal targeting. For example, PCL-colchicine was more effective against HMEC-1 and MS1-VEGF cells compared to the other cell lines. The disruption of microtubules in the endothelial cells was significantly greater for PCL-colchicine compared to free drug, thus making the DOTAP-PCL-colchicine the most suitable candidate for vascular disruption. HMEC-1 has the largest cytoskeleton area and is in fact larger than all cancer cell lines evaluated in this study (Figure 4E). The finding supports the notion that in addition to nanoparticle size and surface charge characteristics, the total cell surface area might represent an important determinant of (vascular) targeting. Given the influence of PCLs on endothelial cell morphology, this factor has a subtle but consequential impact on the general susceptibility of cells to PCL-colchicine [50].

In order to determine whether colchicine was stably incorporated in the PCLs prior to arriving at the tumor target, we designed a dual radiolabeled biodistribution study. This permitted simultaneous tracking of both the vehicle and drug agent. The co-localization study showed that colchicine was delivered via PCLs, and that the natural drug action was likely preserved. Apart from instability due to premature metabolism, colchicine is photosensitive, and when exposed to light the C-ring rearranges to form several analogs which are virtually inactive. It is possible that the protection of colchicine in DOTAP-PCLs shielded the drug from degradation, thus preserving the cellular arrest function of the agent as well [3,8,10,19].

Colchicine is an excellent substrate for P-glycoprotein (PgP), a major contributor to the development of multidrug resistance in tumors (MDR) [51]. The investigation into the effect of colchicine on MDR-sensitive tumor cells was not a goal of the present study. However, the PCL encapsulation of colchicine might well improve the MDR-sensitive (or expressing) cell's level of susceptibility to the effects of the drug. This is due to higher concentration of the drug delivered to the cell. Liposomes in general have previously been employed to overcome MDR for many anticancer drugs [52,53].



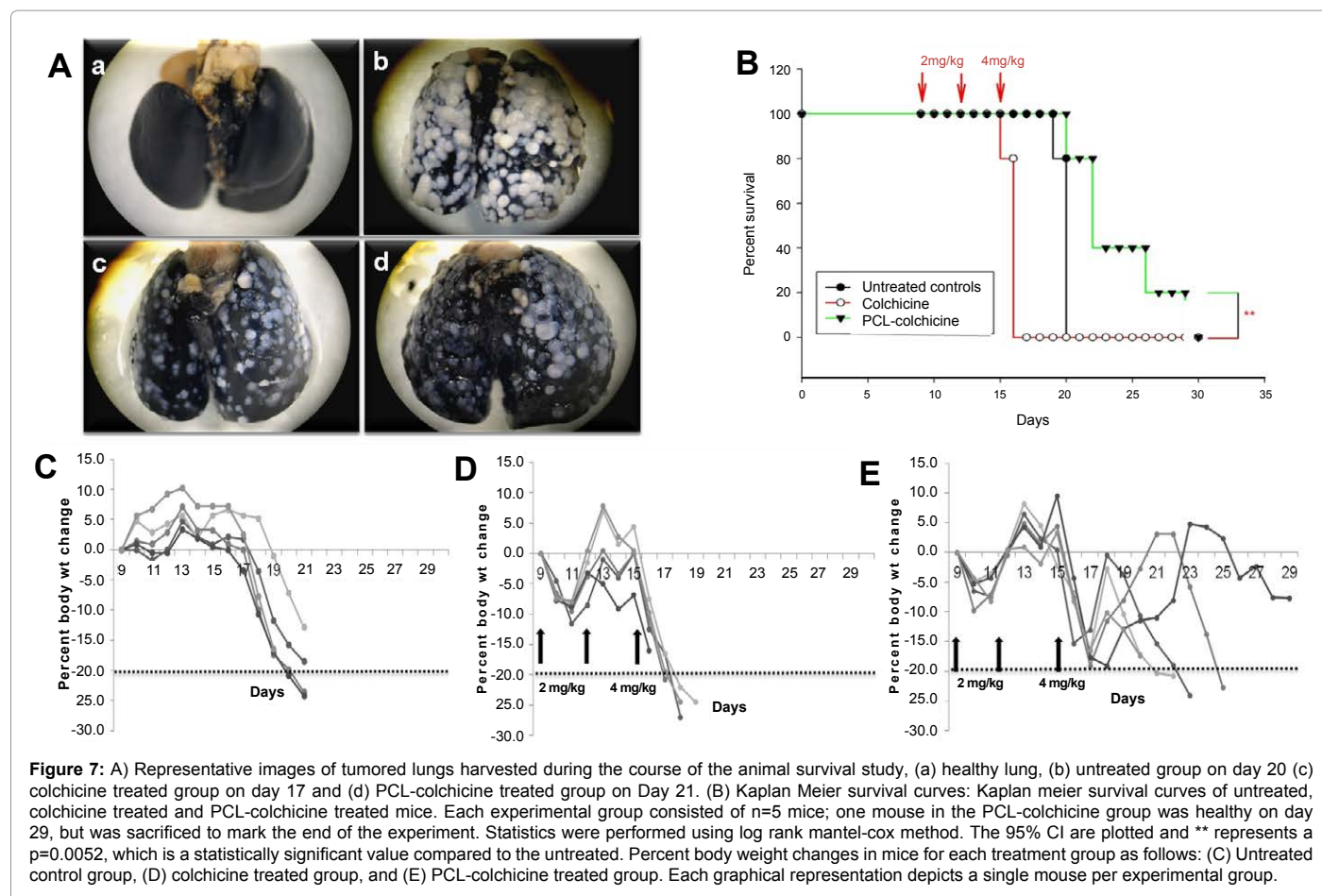
Several lines of evidence support the notion that the pegylation of cationic liposomes improved overall drug plasma retention. This contributed to greater drug uptake by the tumor, and ultimately enhanced the antitumor activity of colchicine. On the other hand, free colchicine was rapidly eliminated from the mice within 3 hrs. It has been reported that 4 mg/kg is the LD₅₀ of the colchicine when administered *i.v.* in mice so the same dose was employed for the survival studies [37]. As expected, all of the mice in the free drug group exhibited definite signs of toxicity, and eventually died 2 days following administration. When the same dose of colchicine was administered in PCLs the mice tolerated the treatment to a greater extent and animal survival was significantly prolonged. Many of the tumor nodules in the treatment groups decreased in size, and in number, when compared to the control group. Colchicine might have arrested the mitosis of rapidly dividing tumor cells resulting in a smaller and reduced number of tumor nodules [3,8,10,19]. The hemorrhage associated with the effect of the free drug was not completely avoided in the PCL-colchicine group, and not all of the mice in the group responded similarly to treatment (Table S3). For this reason, although PCL-colchicine was generally more effective when compared to the free drug, additional formulation and optimization of the dosing and scheduling are required to achieve magic bullet status [54].

Summary

Colchicine incorporates in PCLs with optimal efficiency and stability. PCLs have been shown to enhance the natural cellular arrest function of colchicine, given its antimetabolic activity. The relatively high affinity of the drug carrier for endothelial cells might be attributed to the greater cytoskeletal area of the endothelial cells. The results involving use of the metastatic lung tumor model support the notion that a potent, yet poisonous, clinical agent can be administered in a manner that is relatively safe and effective. These findings collectively support the future development and optimization of PCL-colchicine for cancer therapy.

Acknowledgements

The authors would like to thank Professor Mansoor Amiji at Northeastern University (NEU), Department of Pharmaceutical Sciences, for kindly providing access to the HPLC instrument. We thank Department of Pharmaceutical Sciences for unfettered access to BIOQUANT image acquisition software for quantitative measurements and analysis, at NEU. This article represents work submitted in partial fulfillment of Doctoral degree in Pharmaceutical Sciences, NEU, for first author Dr. Shifalika Tangutoori, PhD. The study was funded in part by the American Association of Colleges of Pharmacy (AACP) New Investigators Program sponsored by the American Foundation for Pharmaceutical Education (AFPE) for R.B.C, and the National Science Foundation CMMI Grant No. 1232339 for R.B.C.



Disclosure statement

The authors have no conflicts of interest.

References

- Siegel R, Ma J, Zou Z, Jemal DVM A (2014) Cancer Statistics, 2014. *CA Cancer J Clin* 64: 1-9.
- Griggs J, Hesketh R, Smith GA, Brindle KM, Metcalfe JC, et al. (2001) Combretastatin-A4 disrupts neovascular development in non-neoplastic tissue. *Br J Cancer* 84: 832-835.
- Hait WN, Rubin E, Goodin S (2005) Tubulin-targeting agents. *Cancer Chemother Biol Response Modif* 22: 35-59.
- Jordan A, Hadfield JA, Lawrence NJ, McGown AT (1998) Tubulin as a target for anticancer drugs: agents which interact with the mitotic spindle. *Med Res Rev* 18: 259-296.
- Tozer GM, Kanthou C, Parkins CS, Hill SA (2002) The biology of the combretastatins as tumour vascular targeting agents. *Int J Exp Pathol* 83: 21-38.
- Zhou J, Giannakakou P (2005) Targeting microtubules for cancer chemotherapy. *Curr Med Chem Anticancer Agents* 5: 65-71.
- Simkin PA (1996) Therapy for gouty individuals. *J Rheumatol* 23: 1115-1116.
- Seed L, Slaughter DP, Limarzi LR (1940) Effect of colchicine on human carcinoma. *Surgery* 7: 696-709.
- Stafford SJ, Schwimer J, Anthony CT, Thomson JL, Wang YZ, et al. (2005) Colchicine and 2-methoxyestradiol Inhibit Human Angiogenesis. *J Surg Res* 125: 104-108.
- Lin ZY, Wu CC, Chuang YH, Chuang WL (2013) Anti-cancer mechanisms of clinically acceptable colchicine concentrations on hepatocellular carcinoma. *Life Sci* 93: 323-328.
- Tortorici MA, Skledar S, Barnes B, Wasko MC (2004) Promoting the safe use of intravenous colchicine. *Am J Health Syst Pharm* 61: 2496, 2501.
- McKeown NJ, Horowitz BZ, Garlich F, Young CR, Robertson WO (2007) Deaths from intravenous colchicine resulting from a compounding pharmacy error - Oregon and Washington, 2007. *Jama-Journal of the American Medical Association* 298: 2364-2366.
- Finkelstein Y, Aks SE, Hutson JR, Juurlink DN, Nguyen P, et al. (2010) Colchicine poisoning: the dark side of an ancient drug. *Clin Toxicol (Phila)* 48: 407-414.
- Deveaux M, Hubert N, Demarly C (2004) Colchicine poisoning: case report of two suicides. *Forensic Sci Int* 143: 219-222.
- Folpini A, Furfori P (1995) Colchicine toxicity--clinical features and treatment. Massive overdose case report. *J Toxicol Clin Toxicol* 33: 71-77.
- Gendron Y, Bronstein JA, Gras C, Boz P (1989) [Neuromuscular toxicity of colchicine. A case]. *Presse Med* 18: 1256.
- Kubler PA (2000) Fatal colchicine toxicity. *Med J Aust* 172: 498-499.
- Fernández S, Castro P, Nogué S, Nicolás JM1 (2013) [Refractory shock and severe leukopenia with multisystemic organ failure due to colchicine intentional overdose.] *J Med Clin (Barc)* .
- Bhattacharyya B, Panda D, Gupta S, Banerjee M (2008) Anti-mitotic activity of colchicine and the structural basis for its interaction with tubulin. *Med Res Rev* 28: 155-183.
- Yue QX, Liu X, Guo DA (2010) Microtubule-binding natural products for cancer therapy. *Planta Med* 76: 1037-1043.
- Crielaard BJ, van der Wal S, Le HT, Bode AT, Lammers T, et al. (2012) Liposomes as carriers for colchicine-derived prodrugs: vascular disrupting nanomedicines with tailorable drug release kinetics. *Eur J Pharm Sci* 45: 429-435.

22. Staropoli N, Ciliberto D, Botta C1, Fiorillo L, Grimaldi A, et al. (2014) Pegylated liposomal doxorubicin in the management of ovarian cancer: A systematic review and metaanalysis of randomized trials. *Cancer Biol Ther* 15: 707-720.
23. Thurston G, McLean JW, Rizen M, Baluk P, Haskell A, et al. (1998) Cationic Liposomes Target Angiogenic Endothelial Cells in Tumors and Chronic Inflammation in Mice. *J Clin Invest* 101: 1401-1413.
24. Kalra AV, RB Campbell (2006) Development of 5-FU and doxorubicin-loaded cationic liposomes against human pancreatic cancer: Implications for tumor vascular targeting. *Pharm Res* 23: 2809-2817.
25. Campbell RB, Fukumura D, Brown EB, Mazzola LM, Izumi Y, et al. (2002) Cationic charge determines the distribution of liposomes between the vascular and extravascular compartments of tumors. *Cancer Res* 62: 6831-6836.
26. Szoka F Jr, Papahadjopoulos D (1980) Comparative properties and methods of preparation of lipid vesicles (liposomes). *Annu Rev Biophys Bioeng* 9: 467-508.
27. Dandamudi S, Campbell RB (2007) The drug loading, cytotoxicity and tumor vascular targeting characteristics of magnetite in magnetic drug targeting. *Biomaterials* 28: 4673-4683.
28. Dabbas SKR, Dandamudi S, Kuesters G, Campbell R (2008) Importance of the Liposomal Cationic Lipid Content and Type in Tumor Vascular Targeting: Physicochemical Characterization and In Vitro Studies Using Human Primary and Transformed Endothelial Cells. *Endothelium* 15: 189-204.
29. Arbisser JL, Larsson H, Claesson-Welsh L, Bai X, LaMontagne K, et al. (2000) Overexpression of VEGF 121 in immortalized endothelial cells causes conversion to slowly growing angiosarcoma and high level expression of the VEGF receptors VEGFR-1 and VEGFR-2 in vivo. *Am J Pathol* 156: 1469-1476.
30. Varsano S, Rashkovsky L, Shapiro H, Ophir D, Mark-Bentankur T (1998) Human lung cancer cell lines express cell membrane complement inhibitory proteins and are extremely resistant to complement-mediated lysis; a comparison with normal human respiratory epithelium in vitro, and an insight into mechanism(s) of resistance. *Clin Exp Immunol* 113: 173-182.
31. Ades EW, Candal FJ, Swerlick RA, George VG, Summers S, et al. (1992) HMEC-1: establishment of an immortalized human microvascular endothelial cell line. *J Invest Dermatol* 99: 683-690.
32. Boui's D, Hospers GA, Meijer C, Molema G, Mulder NH (2001) Endothelium in vitro: a review of human vascular endothelial cell lines for blood vessel-related research. *Angiogenesis* 4: 91-102.
33. Barth RJ Jr, Bock SN, Mulé JJ, Rosenberg SA (1990) Unique murine tumor-associated antigens identified by tumor infiltrating lymphocytes. *J Immunol* 144: 1531-1537.
34. Mukai S, Kjaergaard J, Shu S, Plautz GE (1999) Infiltration of tumors by systemically transferred tumor-reactive T lymphocytes is required for antitumor efficacy. *Cancer Res* 59: 5245-5249.
35. Dandamudi S, Campbell RB (2007) Development and characterization of magnetic cationic liposomes for targeting tumor microvasculature. *Biochim Biophys Acta* 1768: 427-438.
36. BACK A, WALASZEK E, UYEKI E (1951) Distribution of radioactive colchicine in some organs of normal and tumor-bearing mice. *Proc Soc Exp Biol Med* 77: 667-669.
37. Mehta BM, Rosa E, Fissekis JD, Bading JR, Biedler JL, et al. (1992) In-vivo identification of tumor multidrug resistance with 3H-colchicine [corrected]. *J Nucl Med* 33: 1373-1377.
38. Dandamudi S, Patil V, Fowle W, Khaw BA, Campbell RB (2009) External magnet improves antitumor effect of vinblastine and the suppression of metastasis. *Cancer Sci* 100: 1537-1543.
39. Goldfinger SE (1972) Colchicine for familial Mediterranean fever. *N Engl J Med* 287: 1302.
40. Campbell RB, Ying B, Kuesters GM, Hemphill R (2009) Fighting cancer: from the bench to bedside using second generation cationic liposomal therapeutics. *J Pharm Sci* 98: 411-429.
41. Campbell RB (2006) Tumor physiology and delivery of nanopharmaceuticals. *Anticancer Agents Med Chem* 6: 503-512.
42. Immordino ML, Dosio F, Cattel L (2006) Stealth liposomes: review of the basic science, rationale, and clinical applications, existing and potential. *Int J Nanomedicine* 1: 297-315.
43. Abu Lila AS, Kizuki S, Doi Y, Suzuki T, Ishida T, et al. (2009) Oxaliplatin encapsulated in PEG-coated cationic liposomes induces significant tumor growth suppression via a dual-targeting approach in a murine solid tumor model. *J Control Release* 137: 8-14.
44. Cauda V, Engelke H, Sauer A, Arcizet D, Bräuchle C, et al. (2010) Colchicine-loaded lipid bilayer-coated 50 nm mesoporous nanoparticles efficiently induce microtubule depolymerization upon cell uptake. *Nano Lett* 10: 2484-2492.
45. Betageri GV, Hofmann GA, Banga AK (1999) Enhancement of transdermal iontophoretic delivery of a liposomal formulation of colchicine by electroporation. *Drug Delivery* 6: 111-115.
46. Das GS, Rao GH, Wilson RF, Chandy T (2000) Colchicine encapsulation within poly(ethylene glycol)-coated poly(lactic acid)/poly(epsilon-caprolactone) microspheres-controlled release studies. *Drug Deliv* 7: 129-138.
47. Hao Y, Zhao F, Li N, Yang Y, Li K (2002) Studies on a high encapsulation of colchicine by a niosome system. *Int J Pharm* 244: 73-80.
48. Singh HP, Utreja P, Tiwary AK, Jain S (2009) Elastic liposomal formulation for sustained delivery of colchicine: in vitro characterization and in vivo evaluation of anti-gout activity. *AAPS J* 11: 54-64.
49. Kulkarni SB, Singh M, Betageri GV (1997) Encapsulation, stability and in-vitro release characteristics of liposomal formulations of colchicine. *J Pharm Pharmacol* 49: 491-495.
50. Cronstein BN, Molad Y, Reibman J, Balakhane E, Levin RI, et al. (1995) Colchicine alters the quantitative and qualitative display of selectins on endothelial cells and neutrophils. *J Clin Invest* 96: 994-1002.
51. Hendrikse NH, Franssen EJ, van der Graaf WT, Vaalburg W, de Vries EG (1999) Visualization of multidrug resistance in vivo. *Eur J Nucl Med* 26: 283-293.
52. Mamot C, Drummond DC, Hong K, Kirpotin DB, Park JW (2003) Liposome-based approaches to overcome anticancer drug resistance. *Drug Resist Updat* 6: 271-279.
53. Mayer LD, Shabbits JA (2001) The role for liposomal drug delivery in molecular and pharmacological strategies to overcome multidrug resistance. *Cancer Metastasis Rev* 20: 87-93.
54. Fanciullino R, Ciccolini J (2009) Liposome-encapsulated anticancer drugs: still waiting for the magic bullet? *Curr Med Chem* 16: 4361-4371.